

Lithium insertion into hollandite-type TiO_2

Liam D. Noailles¹, Christopher S. Johnson, John T. Vaughey, Michael M. Thackeray^{*}

Electrochemical Technology Program, Chemical Technology Division, Argonne National Laboratory, Argonne, IL 60439, USA

Abstract

Hollandite-type TiO_2 compounds, isostructural with $\alpha\text{-MnO}_2$, have been investigated as insertion electrodes for lithium batteries. Parent materials of $\text{K}_x\text{Ti}_8\text{O}_{16}$ ($0 < x < 2$) were treated with concentrated acid to yield TiO_2 products that were essentially free of potassium. Lithium can be inserted into the (2×2) tunnels of the TiO_2 structure chemically (with *n*-butyllithium) and electrochemically to an approximate composition $\text{Li}_{0.5}\text{TiO}_2$. The lithium ions can be easily removed from the lithiated structure by chemical reaction with bromine; cyclic voltammetry indicates that high voltages are required to remove the lithium by electrochemical methods. The poor electrochemical behavior of hollandite- TiO_2 contrasts strongly with $\alpha\text{-MnO}_2$ electrodes. The superior properties of $\alpha\text{-MnO}_2$ electrodes are attributed to the presence of oxygen ions, either as H_2O or Li_2O , in the (2×2) channels; lithia-stabilized electrodes, $0.15\text{Li}_2\text{O} \cdot \text{MnO}_2$, show good cycling behavior and a rechargeable capacity of approximately 180 mA h/g. © 1999 Elsevier Science S.A. All rights reserved.

Keywords: Lithium battery; Titanium oxide; Hollandite

1. Introduction

Lithium titanium oxides, such as the spinel phase $\text{Li}_4\text{Ti}_5\text{O}_{12}$ [1–3] and the ramsdellite phase $\text{Li}_2\text{Ti}_3\text{O}_7$ [4], have been investigated in the past as possible insertion electrodes for lithium batteries. The spinel phase is of particular interest because three lithium ions can be inserted reversibly into the $\text{Li}_4\text{Ti}_5\text{O}_{12}$ structure at 1.5 V vs. metallic lithium [1]. Although this electrode shows excellent rechargeability and stability, it has a relatively low theoretical capacity (175 mA h/g) compared to TiO_2 (335 mA h/g). The application of TiO_2 compounds as electrode materials, such as rutile, anatase and the spinel LiTi_2O_4 (which reaches a TiO_2 stoichiometry on complete extraction of lithium), has been limited either by their inability to accommodate much lithium or by structural instability to lithium insertion/extraction reactions [5,6]. TiO_2 with a hollandite-type structure is also known to exist; this structure type is normally stabilized by large cations, such as potassium, rubidium [7–9] or thallium ions [10], in the (2×2) channels of the structure, as in the

mineral *hollandite* ($\text{Ba}_x\text{Mn}_8\text{O}_{16}$). These large cations restrict lithium diffusion within the hollandite structure, thereby limiting their usefulness as insertion electrodes. The stabilizing cations can be removed from the hollandite- TiO_2 structure by acid treatment [11] or by reaction with hydrogen peroxide [12]. Recently, it was demonstrated that an isostructural $\alpha\text{-MnO}_2$ material could be synthesized without any stabilizing cation, and that H_2O or Li_2O molecules could be introduced into the (2×2) channels of the structure instead [13]. The lithia-stabilized compound, $\alpha\text{-}[0.15 \text{Li}_2\text{O}] \cdot \text{MnO}_2$, in particular, has shown promising electrochemical behavior; it can provide a rechargeable capacity of approximately 180 mA h/g for many tens of cycles. We have explored the possibility of using a hollandite-type TiO_2 structure without any large stabilizing cation within the (2×2) channels in an attempt to find an electrode with a higher electrochemical capacity to the spinel $\text{Li}_4\text{Ti}_5\text{O}_{12}$.

2. Experimental

Parent $\text{K}_x\text{Ti}_8\text{O}_{16}$ ($1 < x < 2$) samples, alternatively K_yTiO_2 ($0.125 < y < 0.250$), were prepared by heating K_2CO_3 (99 + %, J.T. Baker) and rutile- TiO_2 (99.9 + %, Aldrich) at 960°C for 12 h in 6% hydrogen in helium [14]. Several processing techniques were used to produce sam-

^{*} Corresponding author. Tel.: +1-630-252-9184; Fax: +1-630-252-4176; E-mail: thackeray@cmt.anl.gov

¹ Present address: Inorganic Chemistry Laboratory, Oxford, UK.

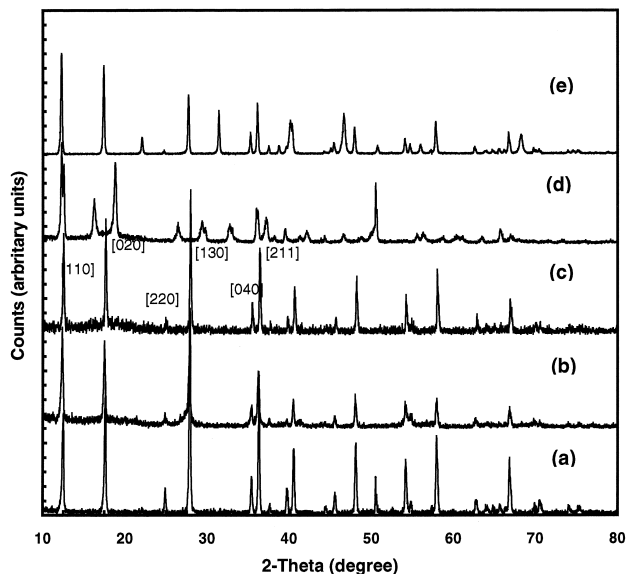


Fig. 1. The powder X-ray diffraction patterns of (a) the parent $K_xTi_8O_{16}$ ($1 < x < 2$); (b) an acid-treated sample, essentially pure TiO_2 ; (c) a chemically prepared sample of nominal composition $Li_{0.125}TiO_2$; (d), a more extensively lithiated sample of composition $Li_{0.57}TiO_2$; and (e) a delithiated sample after treating sample (d) with bromine, with nominal composition Li_yTiO_2 ($0 < y < 0.125$).

ples that were essentially free of potassium: (1) reaction with aqua-regia at 50–100°C [11], (2) reaction with hydrogen peroxide at 80°C [12], and (3) lithium-ion exchange using molten lithium nitrate at 260–340°C. Hollandite-type materials for this investigation were synthesized predominantly by method (1). Lithium was inserted into the hollandite structure chemically (with 1.6 M *n*-butyllithium in hexane at 25°C under argon) and electrochemically. Electrochemical insertion was carried out in button cells (size

1225) of the type $Li/1\text{ M }LiPF_6$ in ethylene carbonate:dimethyl carbonate (50:50)/ Li_xTiO_2 . A detailed description of the cell assembly is presented elsewhere [13]. Cells were discharged and charged at a constant and low rate (0.02 mA/cell). Lithium was extracted from chemically lithiated TiO_2 samples by reaction with a 2-fold mole excess of bromine in chloroform solution at 25°C under nitrogen.

The structures of K_xTiO_2 ($0.125 < x < 0.25$), TiO_2 , and lithiated and delithiated TiO_2 structures were characterized by powder X-ray and neutron diffraction methods. X-ray data were collected on an automated Siemens D-5000 diffractometer with CuK_α radiation. Neutron diffraction data were collected on the General Purpose Powder Diffractometer at Argonne National Laboratory. Refinement of lattice parameters and individual structures was undertaken by a Rietveld refinement using the software program GSAS [15].

3. Results and discussion

The powder X-ray diffraction data of various hollandite- TiO_2 phases are shown in Fig. 1a–e: (a) the parent $K_{0.125}TiO_2$, (b) an acid-treated sample, essentially pure TiO_2 , (c) a chemically prepared sample of nominal composition $Li_{0.125}TiO_2$, (d) a more extensively lithiated sample of composition $Li_{0.57}TiO_2$, and (e) a delithiated sample after treating sample (d) with bromine, with nominal composition Li_yTiO_2 ($0 < y < 0.125$). A refinement of the neutron-diffraction data showed that an acid-leached K_xTiO_2 sample contained a minimal amount of potassium ($< 0.02\text{ K}^+$ per TiO_2 unit), in agreement with a refine-

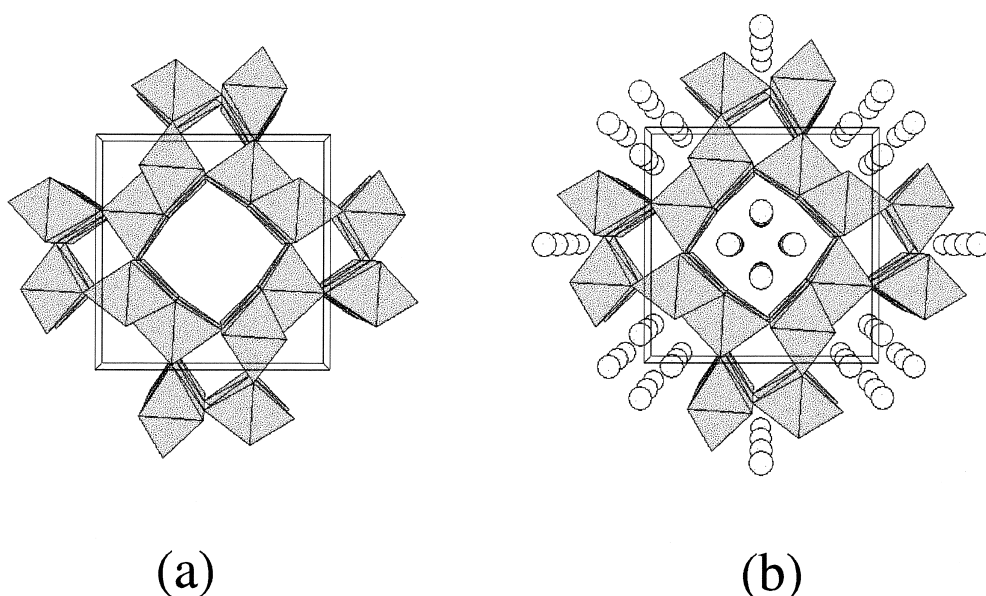


Fig. 2. The structures of (a) hollandite- TiO_2 and (b) a lithiated structure of nominal composition $Li_{0.125}TiO_2$. The lithium atoms are open spheres, and the TiO_6 units are shaded octahedra.

Table 1
Lattice parameters for various hollandite TiO_2 compounds

Compound	a (Å)	b (Å)	c (Å)	β (°)	Volume (Å ³)
$\text{K}_{0.125}\text{TiO}_2$	10.1745(5)		2.9604(2)		306.46(3)
TiO_2 (acid-treated)	10.1534(10)		2.9602(3)		305.18(6)
$\text{Li}_{0.125}\text{Ti}_8\text{O}_{16}$	10.1703(10)		2.9597(3)		306.14(5)
$\text{Li}_{0.57}\text{TiO}_2^*$	14.174(1)	5.436(1)	7.230(1)	97.85(6)	551.8(3)
TiO_2 (Br-oxid)	10.1560(9)		2.9619(4)		305.51(5)

* Proposed monoclinic cell for extensively lithiated hollandite.

ment of the X-ray diffraction data and an energy dispersive X-ray analysis of the sample. The structure of the TiO_2 phase with empty (2×2) channels is shown in Fig. 2a; it is stable in air. A neutron diffraction analysis of a sample with a small amount of inserted lithium, $\text{Li}_{0.125}\text{TiO}_2$, showed that the lithium ions were disordered over crystallographically equivalent sites in the (2×2) channels and coordinated in a distorted tetrahedral arrangement to the oxygen ions at the corners of the channels (Fig. 2b). Although it is likely that such structures will have long-range order, a superstructure or a deviation from the tetragonal symmetry of the parent unit cell ($I4/m$) could not be detected (Fig. 1c). A more highly lithiated sample of composition $\text{Li}_{0.57}\text{TiO}_2$ showed monoclinic symmetry (Fig. 1d); the decrease in symmetry can be attributed to a structural distortion in response to coulombic interactions between the inserted lithium ions in the (2×2) channels, as shown in Fig. 2b. Highly lithiated samples were unstable, particularly when exposed to air; this structural instability has prevented us from undertaking a detailed structural analysis of these samples by neutron diffraction methods. Nevertheless, it has been possible to demonstrate

that lithium can be extracted chemically by water-washing or by treatment with bromine in a nonaqueous solvent from freshly prepared samples of $\text{Li}_{0.57}\text{TiO}_2$ to yield the original TiO_2 phase (Fig. 2b and e).

Table 1 gives the lattice parameters for the various hollandite-type phases of this investigation. Upon removal of the potassium cation from the channel, the [110] and [020] peaks gain intensity relative to the [130] and [211] peaks, and become the most intense peaks in the pattern. Overall, the unit cell is observed to contract in the a/b plane by approximately 0.02 Å, or 0.2%. The volume decreases accordingly, by approximately 0.3%. Lithiation of this empty hollandite framework causes a reversal of the previous changes in both relative peak intensity and unit cell volume. This consistency implies that the volume and lattice shifts are more determined by the slight reduction of the titanium framework than by the specific cation that occupies the channel. Note that the unit cell of $\text{Li}_{0.125}\text{Ti}_8\text{O}_{16}$ is marginally smaller than the potassium compound. Further lithiation produces a more dramatic shift in the pattern as the compound changes to monoclinic ($I2/m$) symmetry. A likely cause of this shift may be

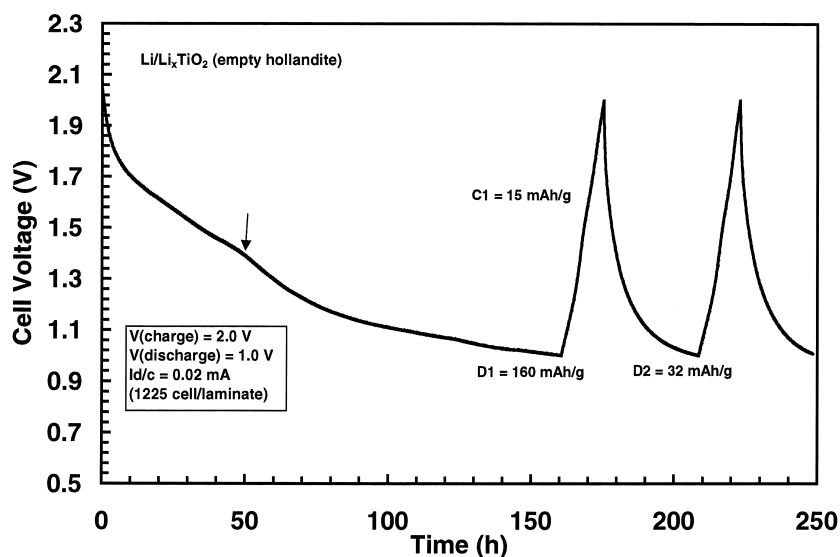


Fig. 3. The voltage profile of a $\text{Li}/\text{Li}_x\text{TiO}_2$ cell showing the initial discharge and the poor electrochemical reversibility of the cell on cycling.

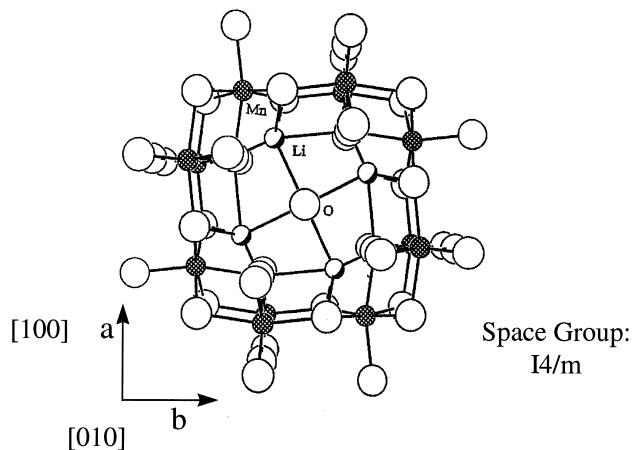


Fig. 4. The structure of lithia-stabilized α - MnO_2 , $0.15\text{Li}_2\text{O} \cdot \text{MnO}_2$, showing the lithium ions coordinated to the oxygen ions of the MnO_2 framework and the oxygen ion that partially occupies a site in the center of the (2×2) channel.

ordering of the lithium cations in the channel due to cation–cation repulsions. Upon delithiation of this sample with bromine, the initial hollandite structure is recovered, with a small amount of LiBr as a by-product of the reaction.

The electrochemical discharge curve (Fig. 3) indicates that at low current rate, lithium is inserted into the TiO_2 structure in two single-phase processes between 2.0 and 1.0 V; the capacity that is delivered on the initial discharge ($\sim 160 \text{ mA h/g}$) corresponds to a discharged electrode composition $\text{Li}_{0.45}\text{TiO}_2$, which is in reasonably good agreement with the composition $\text{Li}_{0.57}\text{TiO}_2$ obtained chemically with *n*-butyllithium ($E^0 \approx 1.0 \text{ V vs. Li}$). Of particular note is the point of inflection at 1.42 V (marked in Fig. 3 with an arrow) in the electrochemical curve (at approximately 30% depth of discharge), which seems to correspond to the transition of the tetragonal unit cell to monoclinic symmetry that occurs during chemical lithiation. The composition of the electrode at this inflection point is $\text{Li}_{0.15}\text{TiO}_2$. With the small amount of residual potassium in the structure, this composition corresponds to the typical amount of stabilizing cation that is found in the (2×2) channels of hollandite- TiO_2 structures, such as $\text{K}_x\text{Ti}_8\text{O}_{16}$ ($1 < x < 2$). Although lithium can be extracted chemically from lithiated TiO_2 structures with bromine (Fig. 1e), it is not possible to easily extract the lithium by electrochemical methods, as is evident by the relatively small capacity that could be recovered on charging the cell to 2.0 V (15 mA h/g) (Fig. 3). Cyclic voltammetry experiments have confirmed the reduction process at 1.42 V, but also indicate a second process at 0.6 V, which is not yet understood. An oxidative sweep to 2.8 V, has shown, however, that both processes are essentially irreversible [16].

The poor rechargeability of hollandite- TiO_2 electrodes contrasts strongly with the behavior of isostructural α -

MnO_2 electrodes [13]. In the manganese oxide system, the hollandite structure is also stabilized by large cations in the (2×2) channels, as in $\text{Ba}_x\text{Mn}_8\text{O}_{16}$ (hollandite) or $\text{K}_x\text{Mn}_8\text{O}_{16}$ (cryptomelane) in which x has a value typically between 1 and 2. However, unlike hollandite- TiO_2 , the α - MnO_2 structure can be stabilized by water (H_2O) or lithia (Li_2O) molecules in the channels. In these stabilized structures, the negatively charged oxygen ion resides close to the site normally occupied by stabilizing cations; this site also corresponds to an oxygen vacancy in a defect close-packed oxygen array [13]. Lithium insertion into lithia-stabilized α - MnO_2 electrodes, notably $0.15\text{Li}_2\text{O} \cdot \text{MnO}_2$, occurs far more readily than it does in the titanium analog because the inserted lithium ions can be coordinated to both the oxygen ions of the α - MnO_2 framework and to the oxygen ion at the center of the (2×2) channels, thus minimizing the coulombic repulsion between the lithium ions. The lithia-stabilized α - MnO_2 structure, shown in Fig. 4, thus provides a more energetically favorable pathway for lithium than hollandite-type TiO_2 structures. The voltage profile of the 20th cycle of a typical $\text{Li}/0.15\text{Li}_2\text{O} \cdot \text{MnO}_2$ cell is shown in Fig. 5a, for comparison; the discharge profile is similar to that of a Li/TiO_2 cell (Fig. 3). However, the $\text{Li}/0.15\text{Li}_2\text{O} \cdot \text{MnO}_2$ cell exhibits good cycling behavior, as shown by the capacity vs.

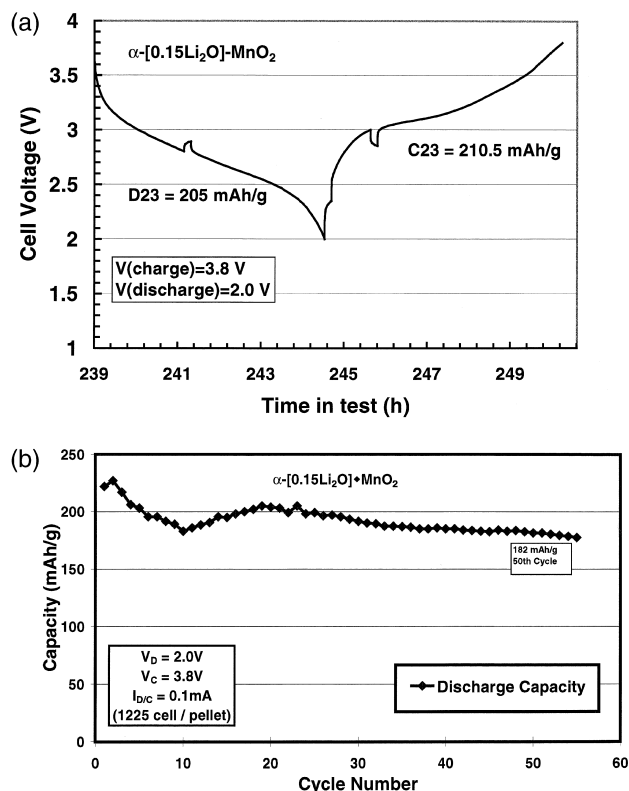


Fig. 5. (a) The voltage profile of a $\text{Li}/0.15\text{Li}_2\text{O} \cdot \text{MnO}_2$ cell at the 23rd cycle and (b) a plot of capacity vs. cycle number for the first 55 cycles.

cycle number plot (Fig. 5b); the $0.15\text{Li}_2\text{O} \cdot \text{MnO}_2$ electrode delivers a capacity of 182 mA h/g after 50 cycles.

4. Conclusions

A hollandite-type TiO_2 structure has been investigated as an insertion electrode material for lithium batteries. This TiO_2 structure is anhydrous and, unlike isostructural $\alpha\text{-MnO}_2$ materials, does not contain water molecules within the (2×2) channels of the structure. The absence of oxygen within the central cavity limits the amount of lithium that can be accommodated within the structure. The inserted lithium ions are strongly bound, in distorted tetrahedral coordination, to the oxygen ions of the framework at the corners of the (2×2) channels, making it difficult to extract the lithium electrochemically from the electrode structure in lithium cells. Hollandite- TiO_2 materials, therefore, appear to have limited use as insertion electrodes for lithium batteries.

Acknowledgements

Support for Argonne National Laboratory from the U.S. Department of Energy's Advanced Battery Program, Chemical Sciences Division, Office of Basic Energy Sciences, under Contract No. W31-109-Eng-38 is gratefully acknowledged.

References

- [1] K.M. Colbow, J.R. Dahn, R.R. Haering, *J. Power Sources* 26 (1989) 397.
- [2] E. Ferg, R.J. Gummow, A. de Kock, M.M. Thackeray, *J. Electrochem. Soc.* 141 (1994) L147.
- [3] T. Ohzuku, A. Ueda, N. Yamamoto, *J. Electrochem. Soc.* 142 (1995) 1431.
- [4] M.E. Arroyo y de Dompablo, E. Morán, A. Várez, F. García-Alvarado, *Mater. Res. Bull.* 32 (1997) 993.
- [5] D.W. Murphy, R.J. Cava, S.M. Zahurak, A. Santoro, *Solid State Ionics* 9–10 (1983) 413.
- [6] Y. Yagi, M. Hibino, T. Kudo, *J. Electrochem. Soc.* 144 (1997) 4208.
- [7] G. Bayer, W. Hoffman, *Am. Miner.* 51 (1966) 511.
- [8] H.U. Beyeler, C. Schüler, *Solid State Ionics* 1 (1980) 77.
- [9] T. Vogt, E. Schweda, C. Wüsterfeld, J. Strähle, A.K. Cheetham, *J. Solid State Chem.* 83 (1989) 61.
- [10] E. Wang, J.M. Tarascon, S. Colson, M. Tsai, *J. Electrochem. Soc.* 138 (1991) 166.
- [11] T. Sasaki, M. Watanabe, Y. Fujiki, *Acta Cryst. B* 49 (1993) 838.
- [12] M. Latroche, L. Brohan, R. Marchand, M. Tournoux, *J. Solid State Chem.* 81 (1989) 78.
- [13] C.S. Johnson, D.W. Dees, M.F. Mansuetto, M.M. Thackeray, D.R. Vissers, D. Argyriou, C.-K. Loong, L. Christensen, *J. Power Sources* 68 (1997) 570.
- [14] M. Watanabe, Y. Koamtsu, T. Sasaki, Y. Fujiki, *J. Solid State Chem.* 92 (1991) 80.
- [15] A.C. Larson, R.B. Von Dreele, GSAS-General Structure Analysis System, Rep. No. LA-UR-86-748, Los Alamos National Laboratory, Los Alamos, NM, 1990.
- [16] C.S. Johnson, unpublished data.